ISSN 0021-8944, Journal of Applied Mechanics and Technical Physics, 2018, Vol. 59, No. 6, pp. 971–979. © Pleiades Publishing, Ltd., 2018.
Original Russian Text © M. Belmahdi, R. Zegadi, S. Simoëns, S. Bouharati.

EXPERIMENTAL INVESTIGATION OF THE FLOW OVER SINGLE AND SUCCESSIVE HILLS ON SMOOTH AND ROUGH WALLS

M. Belmahdi[a], R. Zegadi[a], S. Simoëns[b], and S. Bouharati[c]

UDC 532.5

Abstract: This paper describes a laboratory study of the behavior of turbulent boundary layers in the presence of two-dimensional hills. Flow measurements of the developing turbulent boundary layer on a single hill and on two successive hills are performed in a wind tunnel. The mean and turbulent velocities are measured by PIV anemometry. The results provide a detailed description of the inner layers upstream and above the hills in the separation recirculation zones. The deduced mean and fluctuating velocity fields are compared for the flow in the presence of a single hill and two successive hills located on smooth and rough walls.

Keywords: PIV, two-dimensional hill, recirculation, turbulence.

DOI: 10.1134/S0021894418060020

INTRODUCTION

The main difficulty introduced by steep topographic elevations (hills) is an important nonlinear effect created by the presence of separation in the boundary layer behind a crest summit and formation of recirculation regions. Under these conditions, the prediction of the mean and turbulent fields by the linear theory of Jackson and Hunt [1] is unreliable, which was confirmed by the experiments of Mason and King [2].

Deaves [3] performed some of the earliest numerical modeling studies of boundary layer variation due to changes in roughness and derived empirical formulas for velocities and stresses. The changes in flow behavior caused by the effect of the hill shape and its surface properties were observed by Carpenter and Locke [4]. They quantified the effects of one or more steep hills on the mean and fluctuating velocity of a turbulent flow boundary layer and tested engineering computer programs to predict these effects. By comparing the flow structure on steep and shallow hills, they showed that the flow separation zone downstream of steep hills is larger than that caused by shallow hills. Cao and Tamura [5] studied the effect of surface roughness by comparing the structure of the flow on smooth and rough sinusoidal hills. They found that the recirculation zone reaches further development on rough surfaces. They also mentioned that the inflow conditions have a significant effect on the recirculation zone size.

Almeida et al. [6] are considered as pioneers in describing the behavior of the turbulent field between successive hills. Rapp and Manhart [7] resumed the study by varying the Reynolds number and the distance between the hills. They showed that the length of the recirculation zone behind the second consecutive hill decreases with increasing Reynolds number.

[a]Laboratory of Applied Precision Mechanics, Optic and Precision Mechanics Institute, Setif 1 University, Algeria; miloud_belmahdi@yahoo.fr; rzegadi@yahoo.fr. [b] Fluid Mechanics and Acoustic Laboratory, National Center for Scientific Research, Lyon, France; serge.simoens@ecl-lyon.fr. [c]Laboratory of Intelligent Systems, Setif 1 University, Algeria; sbouharati@yahoo.fr. Translated from Prikladnaya Mekhanika i Tekhnicheskaya Fizika, Vol. 59, No. 6, pp. 15–25, November–December, 2018. Original article submitted April 5, 2018.

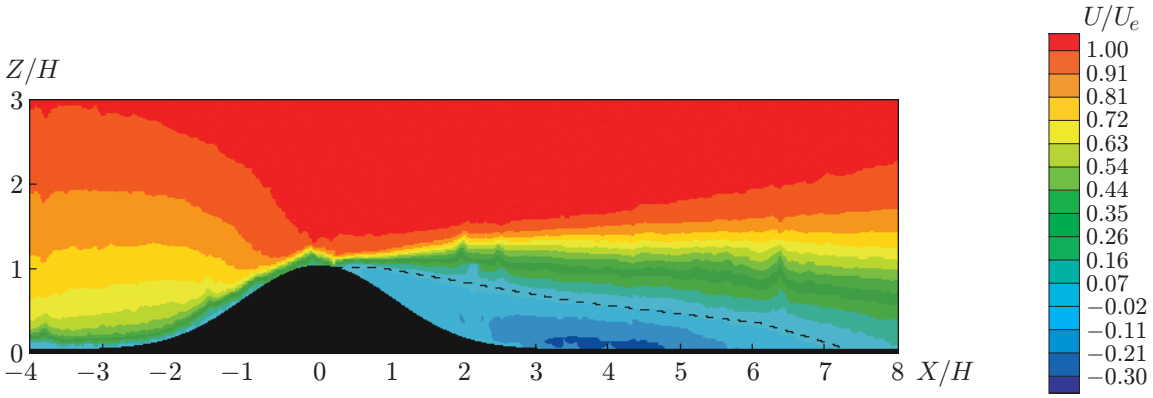

Fig. 1. Velocity field U/U_e for a single hill configuration on a smooth wall: the dashed curve is the line of flow separation.

The main purpose of the present work is to study the flow on steep hills with a separation zone behind their summits. In contrast to [6, 7], where periodic hills were considered, our current research is oriented towards the study of the behavior of a turbulent boundary layer flow on consecutive hills having the same size with different distances between their summits. Both smooth and rough surface states are considered. The effects of these hills on the mean and turbulent characteristics are compared with those of a single hill in three chosen velocity regimes.

1. EXPERIMENTAL PROCEDURE

The flow field in this study is a turbulent boundary layer on a smooth or rough flat wall placed on the median plane at 25 cm above the platform of a wind tunnel installed at the Ecole Centrale de Lyon in France.

The first two-dimensional Gaussian hill is fixed on the wall perpendicularly to the flow direction at a distance of 255 cm from the leading edge (Fig. 1). To initiate and stabilize the laminar-turbulent transition of the boundary layer in the smooth and rough cases, a sandpaper band followed by a 5-mm diameter rod was attached to the wall at 2 cm from the leading edge.

In order to carry out the flow visualization and to obtain quantitative information on the flow structure in the boundary layer, the flow was seeded by an incense smoke injected everywhere at the inlet of the homogenization setting chamber of the wind tunnel. Within the chosen Reynolds number range, the incense particles with a 0.9-μm mean size follow adequately the flow [8]. The Nd-YAG pulsed double cavity laser emitting in the visible range (532 nm) and delivering an energy of 150 mJ per pulse distributed over a 0.5-mm thick sheet by means of a cylindrical lens was used. The frequency of the pulse pairs could reach a value of 4 Hz equivalent to that of the image acquisition time. The images were captured by a single CMOS camera (PCO 4000).

Several preliminary PIV measurements were carried out to verify the characteristics of the turbulent boundary layer on the flat wall induced by the chosen incident flow. Based on previous measurements, three velocity regimes were chosen (U_e = 2.98, 7.92, and 11.20 m/s). These values correspond to Vinçont's validated flow conditions [8] obtained in the same experiment facility (wind tunnel).

In a turbulent boundary layer without obstacles, the mean logarithmic velocity profile over an uniform smooth surface can be defined as

$$\frac{U}{u_f} = \frac{1}{\varkappa} \ln\left(\frac{Z_z u_f}{\nu}\right) + A, \tag{1}$$

and that over a rough surface is defined as

$$\frac{U}{u_f} = \frac{1}{\varkappa} \ln\left(\frac{Z_z}{Z_0}\right),$$

where u_f is the friction velocity, ν is the kinematic viscosity, A is a constant, which varies in the interval 5.0–5.5 for a smooth wall, Z_0 is the ground roughness length, and $\varkappa = 0.41$ is the Kármán's constant. The validity of

Table 1. Characteristics of the boundary layer flow at a distance $x = 255$ cm from the leading edge for different velocity regimes for a single hill on smooth and rough walls

Wall type	U_e, m/s	u_f, m/s	δ, cm	Re_H	Re_θ	Z_d, mm	Z_0, mm
Smooth	2.98	0.113	7.0	1910	1180	—	—
	7.92	0.236	6.5	5077	2580	—	—
	11.20	0.380	5.5	7179	3400	—	—
Rough	2.98	0.142	7	1910	—	195	8.2
	7.92	0.422	7	5077	—	195	8.2
	11.20	0.594	7	7179	—	195	8.2

the logarithmic law can be easily seen by plotting the curve predicted by Eq. (1) as a function of the variables $U^+ = U/u_f$ and $Z_z^+ = Z_z u_f/\nu$ in a semi-logarithmic plot. For denser roughness configurations, the ground is not always the best zero level for the height. It can be argued that an appropriate zero level is located in between the ground and the top of the roughness elements. The zero level is in practice found from wind measurements in the surface layer. It can be defined as $Z_z = Z - Z_d$ (Z is the height above the ground, Z_z is the height above the new zero level, and Z_d is the so-called displacement height). The value of Z_d is expected to be between zero and the average height of the roughness elements, depending on the density and shape of the elements. The modified version of the logarithmic velocity profile is written as

$$\frac{U}{u_f} = \frac{1}{\varkappa} \ln\Big(\frac{Z - Z_d}{Z_0}\Big). \tag{2}$$

The friction velocity u_f and the roughness length Z_0 are obtained by fitting the logarithmic region of the velocity profile (2).

The characteristics of the boundary layer developed in these regimes in the smooth and rough cases at a distance of 255 cm from the leading edge are summarized in Table 1. At this distance, the boundary layer thickness reaches approximately 7 cm. The ratio $H/\delta \approx 1/7$ [9] is one of the main parameters that determine the length of the recirculation zone downstream of the obstacle approximately equal to $7H$. The previous research [6, 8, 9] conducted in the context of a kinematic study in the wake of a two-dimensional obstacle showed that the recirculation extended over a length of about $8H$ downstream of the obstacle, i.e., $H/\delta \approx 1/8$. The rough wall surface is obtained by highly compacted homogeneous solid particles glued together in order to simulate the natural roughness of sandy soils. The particle diameter varies within the range 170–200 μm [9]. The chosen hill geometry (Gaussian shape and size), which can generate a large recirculation region on its lee side, corresponds to that used by Li et al. [10], verifying the typical boundary layer structure. The hill shape is described by the relation

$$X = H\,\mathrm{e}^{-49(Z/H)^2},$$

where $H = 1$ cm represent the hill height. Cut out from a plastic material, the hill was placed at 255 cm from the leading edge. The position and size of our hill correspond to those of Vinçont's obstacle chosen as a cube [8].

The effect of successive obstacles on the boundary layer flow was highlighted by installing a second similar hill at two different distances $L = 3H$ and $L = 8H$ taken between the hills summits. As for the single hill configuration, the same three velocity regimes were used for the smooth and rough cases.

2. RESULTS AND DISCUSSION

Results of an experimental study of the flow over obstacles on smooth and rough walls are reported below.

2.1. Flow in the Presence of a Single Hill on a Smooth Wall

The velocity field of the flow over a single hill on a smooth wall is shown in Fig. 1. The color scale clearly reveals acceleration of the flow above the hill crest. The discontinuous iso-velocity curve represents the separation line determined by the zero mean velocity. The attachment point, corresponding to the intersection of this curve with the wall, occurs at a distance of $0.6H$–$0.8H$, depending on the flow conditions upstream of the hill. It is smaller behind a smooth hill because the flow velocity up at the top is always greater compared to the rough

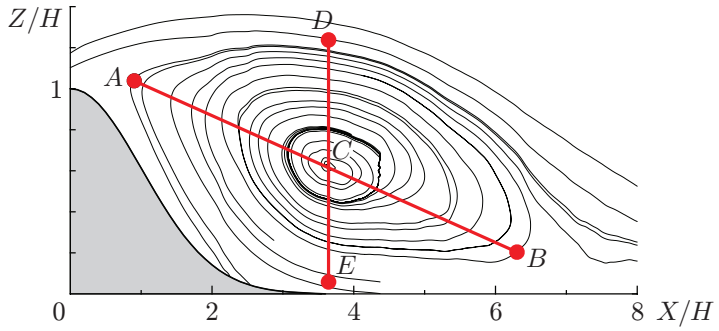

Fig. 2. Recirculation zone behind a single hill on a smooth wall.

Table 2. Characteristics of the recirculation zone formed behind a single hill on smooth and rough walls

Wall type	U_e, m/s	X/H	Z/H	L_{DE}, cm	L_{AB}, cm
Smooth	2.98	3.65	0.58	$0.82H$	$6.15H$
	7.92	3.58	0.59	$0.70H$	$6.80H$
	11.20	3.54	0.59	$0.64H$	$6.90H$
Rough	2.98	3.61	0.58	$1.44H$	$6.15H$
	7.92	3.60	0.61	$1.10H$	$7.35H$
	11.20	3.60	0.62	$0.96H$	$7.50H$

one. As mentioned by Cao and Tamura [11], acceleration of the mean flow caused by the hill slope is accompanied by attenuation of the velocity fluctuations near the wall. This effect confirms that the flow in the smooth case tends to laminarize more rapidly [6, 10].

2.2. Recirculation Zone behind the Single Hill on a Smooth Wall

The size of the separation bubble (recirculation zone) is described by its length and its height, which defines the depth of the deficit region of the momentum exchange. The bubble shape is characterized by the intersecting linear lines L_{AB} and L_{DE} (Fig. 2). The segment AB is the longest segment connecting two ends of the recirculation zone along the downhill slope, and DE is the line representing the thickness of the separation loop passing through the center of this zone and intersecting perpendicularly the extreme external streamline, which is not affected by the separation effect.

The data in Table 2 show the differences between the characteristics of the recirculation zones for different flow regimes over smooth and rough single hills [9].

The coordinates of the recirculation bubble centers behind the hill are practically identical in smooth and rough cases. The distance AB between the separation point behind the hill top and the reattachment point depends on the flow velocity and wall roughness. The length of the vertical segment DE in the rough case is greater than that in the smooth case and decreases with increasing flow velocity, showing recirculation zone flattening. Though the general shape of the recirculation zone is similar on both smooth and rough walls, its size varies greatly in the two conditions. This difference is more perceptible as the flow velocity increases.

2.3. Turbulent Flow on a Single Hill

The vertical profiles of the longitudinal velocity fluctuations normalized by the free stream velocity u'/U_e (u' is the root-mean-square fluctuation velocity) are shown in Fig. 3. A sudden change in u'/U_e is observed on the profile downstream the hill. It is caused by the slightly sheared flow that occurs behind the crest, directed to the flow separation point. Far downstream, the disturbances caused by the hill persist and reach very high values before decreasing due to dissipation and diffusion and returning to the starting level in the upstream flow.

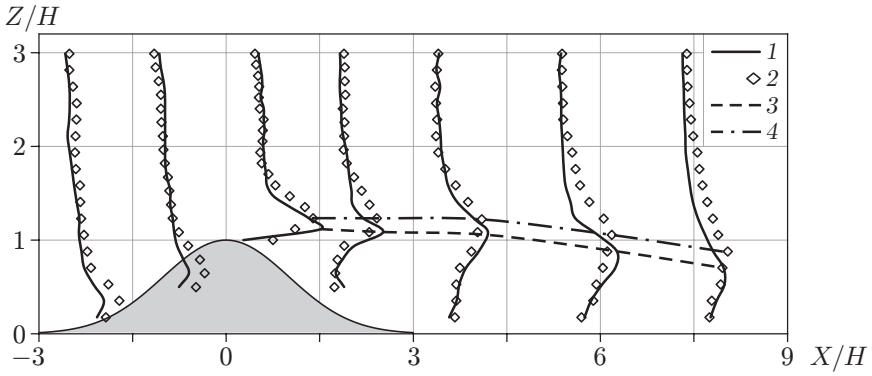

Fig. 3. Profiles of velocity fluctuations u'/U_e (*1* and *2*) and maximum velocity fluctuations $(u'/U_e)_{\max}$ (*3* and *4*) for a single hill on smooth wall (*1* and *3*) and rough wall (*2* and *4*) for the mean flow velocity $U_e = 2.98$ m/s.

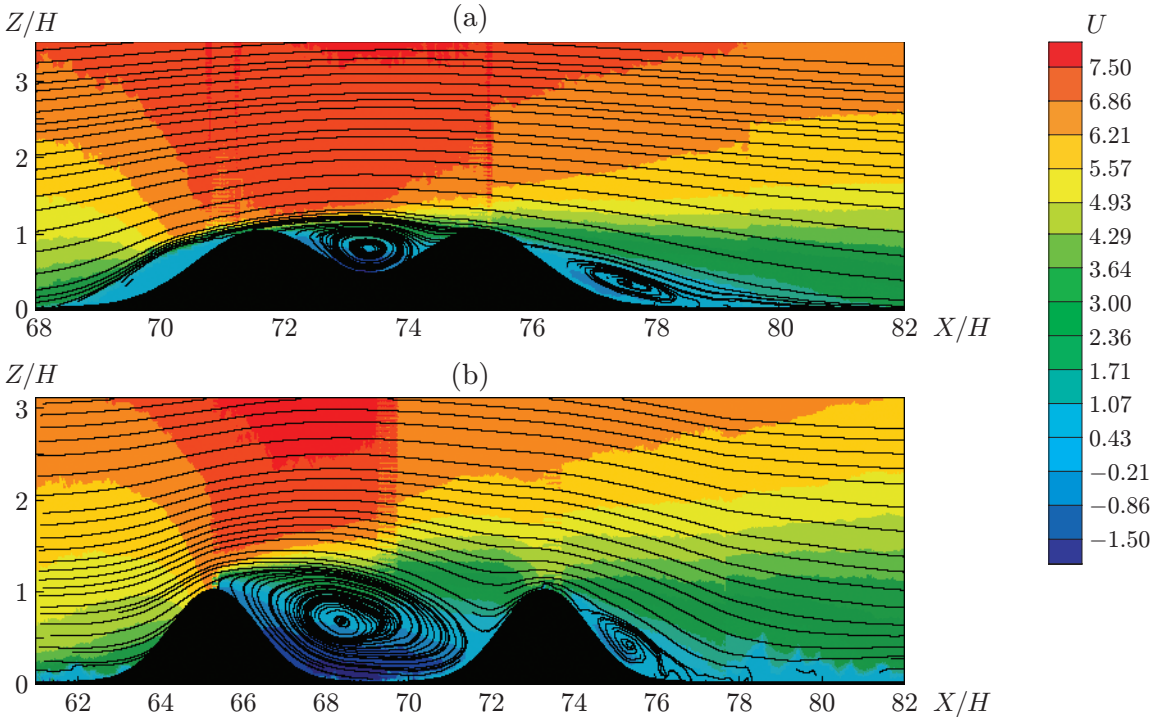

Fig. 4. Flow fields and streamlines for two hills on a rough wall for different distances between the summits and mean flow velocity $U_e = 7.92$ m/s: (a) $L = 3H$; (b) $L = 8H$.

The maximum fluctuating velocity reached in this region is approximately twice the value reached at the hill height in the non-affected flow. The location of this peak is $2H$–$3H$ from the crest for the smooth case and above $3H$ for the rough case.

The discontinuous lines representing, respectively, the positions of the maximum value $(u'/U_e)_{\max}$ on the smooth and rough profiles (see Fig. 3) can be considered as the center of the separated shear layer, which is higher on the rough hill. It is interesting to note that the values of u'/U_e upstream on the rough hill in all velocity regimes are larger than those in the smooth case. However, those on the smooth wall become larger downstream, especially at levels below the hill height. Above the hill height, the values of u'/U_e are larger on the rough wall. This means that the separated shear layer produces a smaller effect on the fluctuating velocity than that in the smooth case.

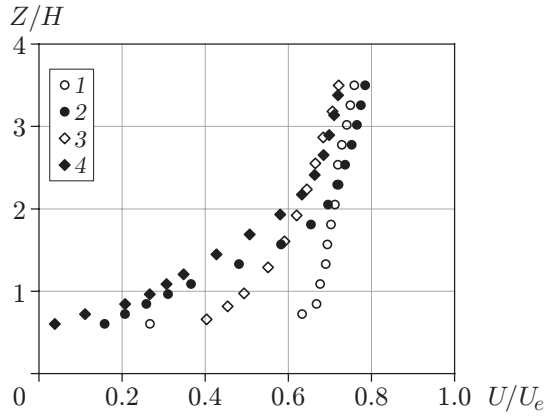

Fig. 5. Mean flow velocities on the upward slopes of two hills for the distance between their summits equal to $8H$ and the main flow velocity $U_e = 7.98$ m/s: points *1* and *2* refer to the first and second hills on a small wall, respectively; points *3* and *4* refer to the first and second hills on a rough wall, respectively.

2.4. Flow in the Presence of Successive Hills

Figure 4 shows the mean streamlines of the flow field for two hills on a rough wall. For the distance between the hill summits $L = 3H$, the center of the recirculation zone is roughly midway between the hills (see Fig. 4a). It is seen that the small area between the hills does not allow significant displacement of the vortex. The stagnation point is located windward near the summit of the second hill. Its position depends on the mean flow velocity.

The outer flow running along the successive hills induces two separation bubbles and forms an envelope with a single hump observed usually for a single obstacle [12]. This is confirmed by the position of the stagnation point, which is practically located at the same level as the hill top. A similar behavior is observed for both smooth and rough situations, although the size of the second recirculation zone appears more pronounced in the smooth case.

The size of the first recirculation bubble in the configuration with $L = 8H$ (see Fig. 4b) is practically not influenced by the surface condition of the hill. However, its thickness depends on the free-stream flow velocity. The flow stagnation point on the second hill rises toward the summit as the free-stream velocity increases. In both smooth and rough wall cases, the second recirculation zone shrinks as the flow velocity increases and tends to move closer to the lee side of the second hill. Its size is generally smaller than that obtained with a single hill. It was reported [13] that the two recirculation bubbles for successive hills become similar to that obtained in a single hill configuration if the distance between the hill tops reaches $4H$ or becomes greater than $12H$.

It follows from Fig. 4 that an increase of the distance between the two hills induces an expansion of the first vortex and deflation of the second one. For the distance between the two hills $3H$, the first recirculation zone remains unchanged in all velocity regimes. In other words, as the stagnation point of the flow on the second hill approaches the summit, the effect of this hill on the recirculation zone size diminishes. The reattachment point of the first recirculation zone in the configuration where the hill tops are separated by a distance $L = 8H$ moves away from the upstream foot of the second hill as the flow velocity increases.

Concerning the second recirculation zone, the size diminishes with the valley distance and flow velocity increasing. Figure 5 shows a decrease in the mean flow velocity on the upward slope near the top when comparing two successive hills in smooth and rough cases in the configuration with $L = 8H$. This velocity decrease is directly related to the second recirculation zone size.

2.5. Turbulent Flow on Successive Hills

As already mentioned, the values of the turbulence intensity for a smooth hill are slightly larger compared to those in the rough case. The peak value in the rough case is always localized at the higher levels.

The velocity fluctuations profiles are similar for all conditions and regimes to those in the single hill configuration.

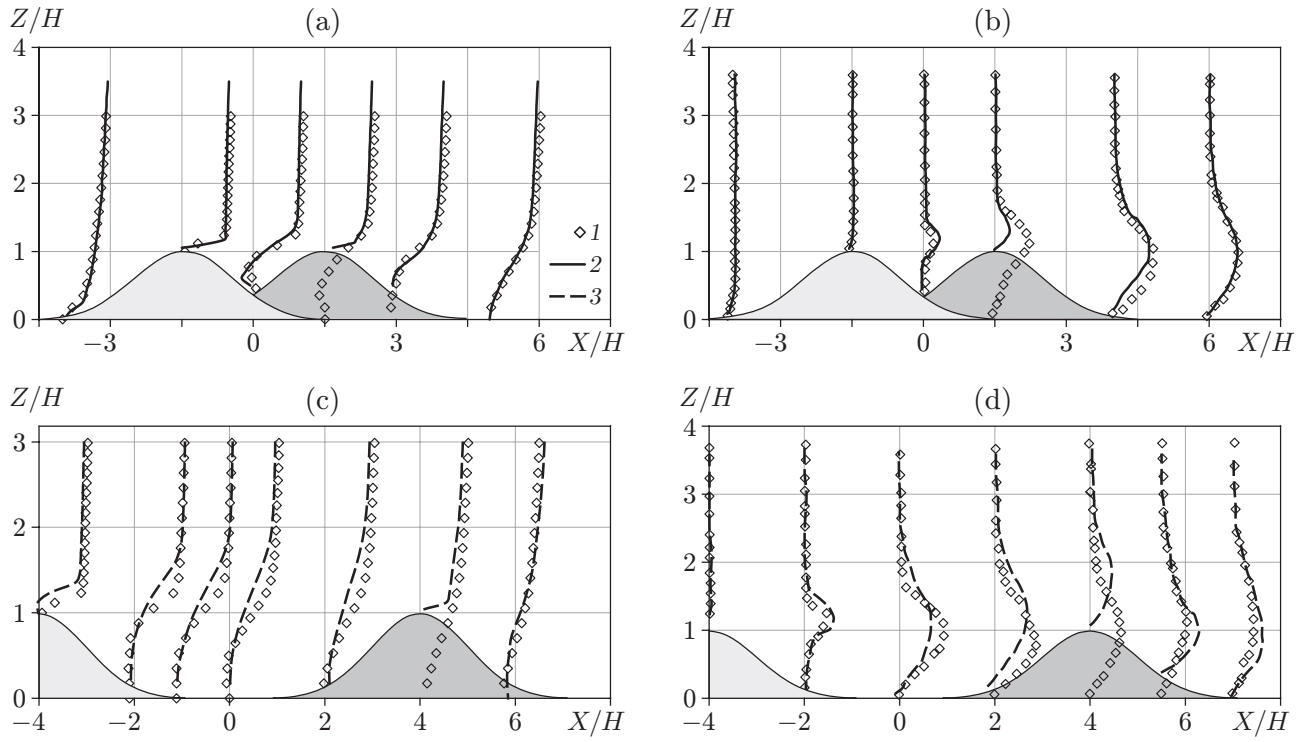

Fig. 6. Mean velocity profiles (a and c) and Reynolds shear stresses (b and d) for the main flow velocity $U_e = 7.98$ m/s for various situations on the rough wall: single hill (*1*), two hills with the distance $3H$ between the summits (*2*), and two hills with the distance $8H$ between the summits (*3*).

The Reynolds stress values for all configurations appear larger in the rough case for all flow velocities. The greatest values in the middle of the valley between the hills are reached at the level $Z/H = 1.2$. A slight blockage of flow by the second hill at the top reduces these values and increases the depth of the sheared layers. In the wake, the Reynolds shear stresses increase again and reach the maximum values at $X/H = 4.5$. At this location, the weak momentum exchange contributes to rising of the sheared flow to the upper layers beyond $Z/H > 2$. The main difference between the Reynolds shear stress behaviors in the configurations with $L = 3H$ and $L = 8H$ is related to the depth of the reversed flow zone (recirculation bubble), which is always greater in the case of the second configuration.

The extent of the sheared layers in the configuration with $L = 3H$ becomes important, but the shear stress value decreases progressively away from the hills. This decrease is more pronounced on rough hills.

Figure 6 shows the mean velocity profiles and Reynolds shear stresses in the rough case for a single hill and two hills with the distance $3H$ between the summits. In the configuration with two hills, the mean flow velocity outside the boundary layer above the first hill crest is smaller than the flow velocity above a single hill (see Fig. 6a). As expected, the Reynolds shear stresses profiles (see Fig. 6b) in the same cross section are identical. Within the separation bubble, these stresses are mitigated by the momentum exchange loss and also by intense flow turbulence. The upward slope of the second hill clearly induces a decrease in the fluctuating velocity. In contrast to the single hill configuration, there is a more than 50% decrease in the Reynolds stress peak values. Downstream the second hill, these stresses are greater than those in the case of a single hill in the profile comprised between the wall and the crest level. Further, in the downstream direction, the flow is still separated, generating shear stresses up to the reattachment point.

The distributions of the mean velocity and shear stress for a single hill and the configurations with the distance $8H$ between the hills are shown in Figs. 6c and 6d. The shear layer in the separation zone on the downstream side of the first hill appears to be less developed than on the single hill (see Fig. 6d). This observation is confirmed by the low velocity gradient between the successive hill feet. At the first foot position ($X/H = -2$),

the peak shear stress $-\overline{u'w'}$ is 10% higher than that found behind the single hill (see Fig. 6d). In the case with two hills, intense vertical mixing occurs. Compared to the single hill, the second hill allows the flow to reattach faster ($X/H = 2$) and appears to have a minor effect on the shear layer above the hill height ($Z/H = 1$).

If the hills are considered as large roughness elements immersed into the turbulent layer, the results obtained in this study prove the existence of three Morris's flow regime categories [14].

In the first flow regime (isolated roughness flow), the roughness element induces a completely developed recirculation zone. In the second regime [flow along a sequence of roughness elements at a small distance ($L = 3H$)], the roughness elements (successive hills) are close to each other so that the first separation bubble does not have enough space to fully develop. In the third regime [flow along a sequence of roughness elements at a large distance ($L = 8H$ in this work and $L = 12H$ in [13])], the recirculation zones created are stable in the space between the hills. According to Morris's investigations [14], the flow observed at $L = 3H$ is comparable to a wake flow and that at the $L = 8H$ behaves similarly to a skimming flow.

CONCLUSIONS

An experimental study of the flow over a single hill and a sequence of hills on a smooth or rough wall is described.

The description of the flow on the single hill reveals an increase in the flow velocity at the top generating a large recirculation zone downstream in all velocity regimes. The size of this zone varies according to the surface roughness and Reynolds number of the flow.

In the configuration with two successive hills with a small distance between them ($L = 3H$), the flow characteristics are globally similar to the flow behind a single hill. The first separation bubble formed between the two hills does not appear to be affected either by the flow regime or by the surface state as a consequence of the limited inter-hill valley distance. The vortex behind the second hill is always smaller because of the closer position of the reattachment point to the hill crest.

In both configurations ($3H$ and $8H$), the fluctuating velocity and Reynolds shear stresses progress from the top of the first hill to reach their peaks midway between the hills. The Reynolds stresses are higher in the rough case than those in the smooth case until the wake formation where they become similar.

Apparently, according to others works, the type of roughness used in this study did not cause any significant effect on the turbulent flow characteristics. The shape of the hills and the flow velocities are the main factors influencing the flow structure.

A comparison of flow characteristics for the configuration with $L = 3H$ with the single hill showed that the successive-hill profiles are nearly identical to the single-hill ones with a slightly higher deceleration across the boundary layer. In the configuration with $L = 8H$, the effect of the increasing distance between the hills is manifested as a significant decrease in the mean velocity and Reynolds shear stress values relative to those measured just behind the single hill. Behind the second hill crest, the profiles become similar.

REFERENCES

1. P. Jackson and J. Hunt, "Turbulent Wind Flow over a Low Hill," Quart. J. Roy. Meteorol. Soc. **101**, 929–955 (1975).
2. P. Mason and J. King, "Measurements and Predictions of Flow and Turbulence over an Isolated Hill of Moderate Slope," Quart. J. Roy. Meteorol. Soc. **111**, 617–640 (1985).
3. D. Deaves, "Computations of Wind Flow over Two-Dimensional Hills and Embankments," J. Wind Eng. Indust. Aerodynamics **6**, 89–111 (1980).
4. P. Carpenter and N. Locke, "Investigation of Wind Speeds over Multiple Two-Dimensional Hills," J. Wind Eng. Indust. Aerodynamics **83**, 109–120 (1999).
5. S. Cao and T. Tamura, "Experimental Study on Roughness Effects on Turbulent Boundary Layer Flow over a Two-Dimensional Steep Hill," J. Wind Eng. Indust. Aerodynamics **94**, 1–19 (2006).
6. G. Almeida, D. Durao, and M. Heitor, "Wake Flows Behind Two-Dimensional Model Hills," Experiment. Thermal Fluid Sci. **7**, 87–101 (1993).

7. C. Rapp and M. Manhart, "Flow over Periodic Hills: An Experimental Study," Exp. Fluids **51**, 247–269 (2011).
8. J. Y. Vinçont, S. Simoëns, M. Ayrault, and J. Wallace, "Passive Scalar Dispersion in a Turbulent Boundary Layer from a Line Source at the Wall and Downstream of an Obstacle," J. Fluid Mech. **424**, 127–167 (2000).
9. S. Simoëns, S. Saleh, C. Leribault, et al., "Influence of Gaussian Hill on Concentration of Solid Particles in Suspension Inside Turbulent Boundary Layer," Procedia IUTAM **17**, 110–118 (2015).
10. Q. Li, T. Maeda, Y. Kamada, and K. Yamada, "Experimental Investigation of Flow over Two-Dimensional Multiple Hill Models," Sci. Total Environment. **609**, 1075–1084 (2017).
11. S. Cao and T. Tamura, "Effects of Roughness Blocks on Atmospheric Boundary Layer Flow over a Two-Dimensional Low Hill with/without Sudden Roughness Change," J. Wind Eng. Indust. Aerodynamics **95**, 679–695 (2007).
12. J. C. Kaimal, *Atmospheric Boundary Layer Flows: Their Structure and Measurement*, Ed. by J. C. Kaimal and J. J. Finnigan (Oxford Univ. Press, Oxford, 1994).
13. A. Ferreira, M. Silva, D. Viegas, and A. Lopes, "Wind Tunnel Simulation of the Flow Around Two-Dimensional Hills," J. Wind Eng. Indust. Aerodynamics **38**, 109–122 (1991).
14. H. M. Morris, "Flow in Rough Conduits," Trans. ASME **120**, 373–398 (1955).